Visualizing sunsets through inhomogeneous atmospheres

F. J. Seron, D. Gutierrez, G. Gutierrez, E. Cerezo

Grupo de Informática Gráfica Avanzada (GIGA)
http://giga.cps.unizar.es
Departamento de Informática e Ingeniería de Sistemas
Centro Politécnico Superior - Universidad de Zaragoza
María de Luna 1, 50018 Zaragoza (Spain)

seron@unizar.es, diegog@unizar.es,
guillermof@unizar.es, ecerezo@unizar.es

Abstract

In this paper, it is described a method of curved ray tracing capable of depicting phenomena that arise, under certain conditions, when light propagates through an inhomogeneous atmosphere. As an example application the distortions in the spherical shape of the sun during sunsets are modelled, including split suns, flattened suns and double suns. Nevertheless, the method is general and can be applied to any media in which the index of refraction is a function of the position.

1. Introduction

The modelling of nature scenes is one of the most ambitious goals of the Computer Graphics community [1]. There have been several examples that simulate the behaviour of light within the atmosphere, for example, the doctoral thesis of Musgrave [2] or the work of Berger and Trout [3], which studies the phenomenon of light scattering in the atmosphere.

Up to now, most of the ray-tracing algorithms consider that light is propagated following straight lines. This is so because these algorithms presuppose either that there are no media through which the light travels, or that these media are homogeneous, that is, they have the same properties in all their points. However, most media are inhomogeneous, with properties varying continuously from point to point. For instance, the atmosphere is in fact an inhomogeneous medium, because the pressure, temperature and other properties vary from point to point, and so, its optical characteristic defined by the index of refraction is not constant in all the points.

There are some previous works on the subject of curved ray tracing in inhomogeneous media, as well as papers talking about non-linear ray tracing. Among the former, we can mention [4], [5] and [6]. The first two, however do not present a generic situation in which the index of refraction varies throughout the atmosphere in an arbitrary way, and in fact focus only on mirages. While the approach in [6] is more closely related to ours, our method of resolution is different and more general.

Berger and Trout [4] are the first ones to observe that the ray tracing method only changes the trajectory of the ray when it intersects an object. Therefore, the slight changes in direction that rays experiment when going through the atmosphere were not considered. Those changes are, precisely, the origin of the mirages. According to Fermat's law, light crossing a medium gets curved towards the areas with a greater index of refraction. The index of refraction of the air depends on both humidity and density, but the effect of the former on light is very small and can be ignored. On the contrary, density, which is a function of pressure and temperature, can significantly change the light rays' trajectories. In the case of the mirage effects, these occur in a very small altitude range, where pressure is practically constant; therefore, the change in the index of refraction can be supposed to be owed only to temperature variations. In their work, they solve the problem dividing the medium into various homogeneous layers. The proposed solution is to subdivide the atmosphere in multiple horizontal layers with a different index of refraction for each one. When using ray tracing, the ray launched from the observer is refracted every time it crosses a boundary between

Proceedings of the Computer Graphics International (CGI'04)
1530-1052/04 $20.00 © 2004 **IEEE**

layers. This method is then only valid for situations where the index of refraction is only a function of the height; on the other hand, it is impossible to obtain the real curved path followed by the ray, coming up instead with an approximation made of straight segments.

Musgrave [5] points out a few considerations regarding the interpretation of the model in [4] and its implemented version. He indicates that the primary bending agent in the formation of mirages is total reflection, instead of refraction as is proposed in [4]. As a consequence, a purely reflective model might suffice, without the need for refraction. Musgrave reinforces this idea by stating that, if refraction were the primary engine in mirage formation, one would then expect to see the effects of dispersion in a mirage, smearing the image into its component colours. On the contrary, there is little to no dispersion in mirages observed in nature.

Stam and Languénou [6] present their work on ray tracing in non-constant media. They do not use Snell's law to calculate the trajectory of the light ray, unlike the previous works described. On the contrary, they obtain the differential equation that describes the trajectory of the ray from the equation of the light wave, coming to the following expression:

$$\frac{d^2}{dl^2}\vec{r}(l) = \frac{1}{2}\nabla n(\vec{r}(l)) \qquad (1)$$

where l is the arc's length, n is the index of refraction and $\vec{r} = x_j$ (j = 1,2,3) are the coordinates of a given point. In [6] they also observe that the index of refraction of the atmosphere is inversely proportional to the temperature of the air:

$$n = 1 + \frac{T_0}{T}(n_0 - 1) \qquad (2)$$

where T_0 = 273 and n_0 = 1.00023.

For a given hot horizontal surface at a temperature T_s, the temperature above it has an exponential falloff characterized by the attenuation distance d_0. Using equation 2, the expression for the index of refraction would be the following:

$$n(\vec{x}) - 1 = \frac{T_0(n_0 - 1)}{T_0 + (T_s - T_0)\exp(-(\vec{x} - \vec{o}).\vec{n} / d_0)} \qquad (3)$$

where the hot horizontal surface is defined by its origin $\vec{o}$ and its normal $\vec{n}$. If the attenuation distance is big enough, the rays follow approximately a parabolic trajectory, and the method described in [4] yields good results. However, if the attenuation distance is small, the trajectories become hyperbolic, and the approximation in [5] works better by using total reflection.

To solve equation 1, Stam and Languénou propose a perturbation method [7], and apply it to two particular cases. The first one consists on a superposition of *N* hot nuclei, whereas in the second one the distributions of the index of refraction are defined by a stochastic model, that is, Fourier's transform of a random index of refraction.

On the other hand, Groeller [8] considers different situations that cause non-linear paths. These can be the result of underlying dynamic systems that act upon a particle, such as gravity centres, gravity lines or dynamic chaotic systems, or can be defined arbitrarily in a explicit manner through equations. In the first case, the curved rays are the solutions of first-order ordinary differential equations, that is, $\vec{x}' = V(\vec{x})$ with an initial value $\vec{x}_0$. Usually, the exact solution $\vec{x} = \vec{x}_0 + \int \vec{V}(\vec{u})d\vec{u}$ cannot be calculated analytically. It is then necessary to use numerical techniques, and he chooses Euler's method to calculate successive points of the curve path knowing the position and the tangent vector at the previous point.

To calculate the position and velocity of a point in the curved trajectory $(\vec{x}_{n+1}, \vec{v}_{n+1})$, knowing the position and velocity in the previous point $(\vec{x}_n, \vec{v}_n)$, the following equations are used:

$$\vec{x}_{n+1} = \vec{x}_n + \Delta l \cdot \frac{\vec{v}_n}{\|\vec{v}_n\|} \qquad (4)$$
$$\vec{v}_{n+1} = f(\vec{x}_n, \vec{v}_n)$$

where Δl is the integration step and $f(\vec{x}_n, \vec{v}_n)$ is the function to obtain the velocity in the next point. As it has been said before, it can be based on physical laws or be arbitrarily defined.

Another problem, inherent to curved ray tracing and light, is obtaining the trajectory that goes from the intersection point to a light source. Here, Groeller proposes two possible solutions. The first one consists of supposing that the light rays are only curved from the intersection point to the eye, but travel in a straight line from the light source to the intersection point. The second one consists of assigning color to the intersection point regardless of the light sources, for instance by using textures with the illumination pre-calculated.

The method proposed in this work has none of the limitations that appear in the articles previously discussed, regarding the dependences of the index of refraction function. This is so because we solve the problem of light propagation through an inhomogeneous media using the general equation, based on Fermat's principle, that describes the phenomenon [9] [10]:

$$\frac{d}{dl}\left(n\frac{d\vec{r}}{dl}\right)-\nabla n=0 \leftrightarrow \frac{d}{dl}\left(n\frac{dx_j}{dl}\right)-\frac{\partial n}{\partial x_j}=0 \quad (5)$$
(j=1,2,3)

where l is the length of the arc, n is the index of refraction of the medium and $\vec{r}=x_j$ with (j=1,2,3) are the coordinates of the point.

This way, we can reproduce any of the previous works while broadening the scope of possible applications. Even though the proposed resolution method is general, it is going to be applied here only to atmospheric phenomena, specifically to simulate distortions of the spherical shape of the sun during sunsets (including the split sun, the flattened sun and the double sun).

The structure of this paper is as follows: in section 2, we present a numerical method for the resolution of the problem posed by equation 5 as well as its convergence. In section 3, to be able to compare the behaviour of the method, we offer the exact solution and two approximate solutions in the special case of an atmosphere with linear variation with height of its index of refraction. In section 4, we visualize the sunset phenomena enumerated before. Finally, in section 5, we comment on the conclusions, while future work is discussed in section 6.

2. General method of resolution of the path equation

The method to calculate the path of the ray in a general case in which the index of refraction in all the points of the medium is known, consists of calculating the index of refraction and the slope of the curve at step i, advancing a length Δl_i along the direction of the tangent of the curve to reach step $i+1$, and then calculating the new index of refraction and the direction of the slope of the path at step $i+1$. Then, advancing a length Δl_{i+1} along the new direction of the tangent and so on until we get to the intersection point of the path of the ray with an object.

For each step, it is necessary to calculate the direction of the tangent. To do this, we calculate a numeric approximation through a discretization of equation 5, that is, replacing differentials by increments and applying Euler's method. If we use x_{ji} for the coordinate j of the point of the ray at step i and x_{ji+1} for the coordinate j of the point of the ray at step $i+1$ we get:

$$n_{i+1}\frac{dx_{ji+1}}{dl}-n_i\frac{dx_{ji}}{dl}=\frac{\partial n}{\partial x_j}\Delta l_i \quad (6)$$

So, if we know n_{i+1}, n_i, $\frac{dx_{ji}}{dl}$, $\frac{\partial n}{\partial x_j}$ and Δl_i it is possible to obtain the slope of the curve $\frac{dx_{ji+1}}{dl}$:

$$\frac{dx_{ji+1}}{dl}=\frac{n_i\frac{dx_{ji}}{dl}+\frac{\partial n}{\partial x_j}\Delta l_i}{n_{i+1}} \quad (7)$$

Given an estimate of the tolerable error, the optimum integration step can be selected for each instant. To do this we use the Richardson extrapolation algorithm. Although Euler is a first-order method, this process assures the convergence (stability plus consistency) of the method [11] even in the cases in which sharp variations in the index of refraction occur. This is so because the method fits the integration step to the characteristics of the problem in such a way that the accuracy obtained is inferior to a prefixed tolerance.

3. Behaviour of the general method through comparison with less general methods

We are going to analyse the behaviour of the general method, in terms of speed and accuracy. To do so, we are going to compare it with three less general methods for the special case of an atmosphere which index of refraction varies linearly with height.

3.1. Exact method

We define a medium which index of refraction varies linearly with height, that is, the index of refraction verifies:

$$n(y) = n_{mid} + (n_{\sup} - n_{mid})\frac{y}{h} \qquad (8)$$

where n_{mid} is the value of n at the middle level (for $y=0$), $n_{\sup}$ is the value of n at the upper level (for $y=h$) and the function $n(y)$ valid from $y=-h$ to $y=h$.

The solution of the differential equation allows to express the path of the ray as a function of the parameter l (length of the curve).

3.2. Rough methods

We propose the following rough methods that can be used to obtain an estimate of the result:

Rough method 1: we can think about dividing the medium into various horizontal layers with a constant index of refraction. In this way, to calculate the path, we have just to apply Snell's law of refraction when the ray is going to change layers. For those cases in which the refracted ray does not exist, we calculate the reflected ray. This is the same method used by Berger and Trout [4] to calculate images of mirages.

Rough method 2: the drawback to the solution proposed by the rough method 1 is that rays that follow almost an horizontal path need to travel a great distance before significantly changing direction. This can be improved by calculating the refracted ray when it has travelled a fixed distance l. In this way, the more horizontal the ray, the thinner the layers become.

3.3 Test scenes

We are going to analyse the different methods proposed, computing the errors and rendering times using four different scenes. The four scenes are identical and the distribution of the index of refraction n always follows equation 8, but the value at the lower and upper levels varies as described in Table 1. The values we have used for the test scenes to set the index of refraction fall within the range of values found in the atmosphere.

Table 1. Description of the four test scenes

	n(-h)	n(h)
Scene I	1.0	1.02
Scene II	1.02	1.0
Scene III	1.0	1.5
Scene IV	2.0	1

We must emphasize that, in order to test the proposed methods, neither the geometry of the scene nor the output image size are important parameters. What is being studied here is the curvature of the rays travelling a long distance. Thus, the parameter that will really give us meaningful data is the size of the scene (made up of two infinite planes), hence the geometrical simplicity. Parameter h has a value of 50 units and the rendered image has a size of 100 by 100 pixels. The coordinates of the points at the viewport window range from -50 to 50 units both in x and y and the camera is placed 100 units in front of the image plane. The scene is composed of a horizontal infinite plane located at $y=-h$ as the ground and a horizontal infinite plane located at $y=h$ as the sky.

3.4. Comparison of the methods

For each method (the general method explained in section 2, plus the exact and rough methods 1 and 2 of this section), we calculate the elapsed time: it is the time necessary to generate the scenes using a Sun Sparc Station at 100 MHz.

In the comparison, we use rough method 1 with three different subdivision levels (different number of layers), and rough method 2 and the general method with two different preset values of l (the distance travelled along the curve before calculating its change of direction, measured in length units). For the general method, the Richardson extrapolation algorithm has also been used in a third test to obtain this parameter at each step, as explained in section 2. The results obtained are shown in Tables 2 and 3.

The method of uniform subdivision of space (rough method 1) is the one with the poorest results error-wise, so it should not be used in practice.

The method of non-uniform subdivision of space (rough method 2) takes roughly twice as long as the general method based on equation 5 for a given, fixed integration step.

The general method with l obtained through Richardson extrapolation algorithm is almost four times slower than the same method with l preset to a fixed value of 0.5, and about seven times slower with the fixed value of 1. This is owed to the greater number of calculations that need to be done in order to obtain each integration step. This aspect is merely circumstantial, though, owed to the necessity to compare the methods in this paper. In a real-life problem with a variable index of refraction, the adequate value of l is not usually known beforehand.

Table 2. Rendering time (in seconds) for the four test scenes using the four different methods

		Scene I	Scene II	Scene III	Scene IV
Exact method		2.3	2.3	2.1	2.1
Rough meth. 1	100 lay.	17.5	17.4	18.4	17.4
	500 lay.	89.5	88.2	90.0	85.1
	1000 lay.	183.1	199.0	180.6	170.5
Rough meth. 2	l=1	119.9	119.5	56.3	43.8
	l=0.5	249.6	239.5	112.4	87.2
General method	l=1	59.2	59.2	28.2	22.0
	l=0.5	118.7	118.1	56.3	43.4
	Richardson	412.0	414.8	196.0	186.2

Table 3. Average error in the x coordinate of the pixels

		Scene I	Scene II	Scene III	Scene IV
Exact method		0	0	0	0
Rough meth. 1	100 lay.	4.7	5.4	4.9	4.6
	500 lay.	1.7	2.1	1.7	1.4
	1000 lay.	1.2	1.9	1.1	0.9
Rough meth. 2	l=1	0.08	0.08	0.21	0.23
	l=0.5	0.03	0.04	0.11	0.11
General method	l=1	0.10	0.13	0.13	0.13
	l=0.5	0.07	0.03	0.06	0.07
	Richardson	0.08	0.11	0.05	0.05

We must also emphasize that only the general method could be applied to a complex situation in which we had defined the index of refraction corresponding to a general inhomogeneous medium.

4. Animation of sunsets

As it has been stated before, the atmosphere is clearly an inhomogeneous medium. This is so because the density of the air is usually greater the closer to the earth. As the density of the air decreases with height, the index of refraction also decreases. We are going to depict here different situations that may arise due to differences in the index of refraction of the atmosphere.

More precisely, we are going to model the distortions of the spherical shape of the sun during sunsets. We have generated animations of sunsets under certain distributions of the index of refraction of the atmosphere. Three different phenomena that may arise when watching a sunset are going to be depicted: the split sun, the flattened sun and the double sun [7].

To generate the animations for the sunsets, we have used astronomically precise dimensions. Our scene is made up of a black sphere of 6375 length units of radius representing the earth (here the units can be thought of as being kilometres). Another sphere of 695000 units of radius represents the sun. The distance between the spheres is 150 million units. The observer is located at a small distance above the surface of the earth. We have also added several triangles over the surface of the earth to simulate irregularities over it.

4.3.1. Split sun

It is a curious phenomenon that may arise when there is a cold air layer near the earth and a warmer layer above it. The phenomenon of total reflection may take place when a ray passes from one medium to another with a smaller index of refraction with an adequate angle. In that situation there is no refracted ray, and the ray is reflected.

In Figure 1.a we have represented the earth and the layer of discontinuity, and we have traced three rays from the observer *O*. In Figure 1.b, we show the distribution of the index of refraction used. The index of refraction only depends on the distance from the point to the centre of the earth (radial coordinate). This distribution causes the split sun effect, with two portions of the sun separated by an empty strip located around the horizontal plane that passes through the observer. Figure 1.c shows several frames of the resulting simulation. In Figure 1.d a real picture of the effect can be seen.

4.3.2. Flattened sun

This is the most common case that appears in an atmosphere in which the index of refraction decreases with height, because the density of the air decreases as one moves away from the earth, and so the index of refraction decreases as well. As a result of this, the sun is not seen as a perfect circle, but appears rather flattened along the vertical axis. This happens because the rays become curved downwards, towards the areas with a greater index of refraction (see Figure 2.a). This causes a distortion of the image we receive from the sun. Moreover, the image of the sun appears higher than it should. Figure 2.b shows the distribution of the index of refraction for this scene, while Figure 2.c shows several frames of the results obtained. A real picture of the effect is shown in Figure 2.d.

4.3.3. Double sun

This is the phenomenon that takes place when there is a very thin layer of warm air over the surface of the earth. In this case, the rays traced from the observer, that do not make contact with the ground are not affected by the warm layer. Therefore, the sun is perceived without distortion. However, the rays which do make contact with the warm layer become curved upwards. As a consequence, part of them intersect again with the sun, and as a result, we perceive a double image of the sun.

The effect is explained in Figure 3.a. Figure 3.b shows the distribution of the index of refraction for this case. To add realism, we have also included a decrease of the index of refraction as a function of height. Figure 3.c shows several frames of the resulting animation while in Figure 3.d a real picture of the effect can be seen. The difference between the effect generated through curved ray tracing and the real one is owed to the thickness of the warm layer and the position of the sun relative to the observer. Different combinations of these two parameters yield different outputs based on the same double-sun effect.

4.5. Implementation details

The values chosen for the indexes of refraction are not really important; only the relative difference between the values in all the points matters. That is, we could double or half the values in all the points to obtain the same results. Despite this, the values we have used are the values we can find in nature. It is also worth mentioning the fact that slow variations in the index of refraction require big scenes in order for the effects to be visible.

As explained by Groeller [8], simulating the lighting through light sources would involve tracing a curved ray from the intersection with the geometry to the light source. Here, the colours have been obtained directly from real photos instead, as proposed in [8], which is a much simpler process. This decision is justified by the facts that the geometry of the scene is very simple, and there is no artificial or secondary light sources that would contribute to the lighting.

The scenes have been generated using the T3E [12] computers of the Edinburgh Parallel Computing Centre (EPCC) of the University of Edinburgh. The T3E is composed of 256 Alpha EV 5.6 processors with 128 Mb of memory and 900 Mflops of peak performance each one, although only a maximum of 64 processors can be used.

Resorting to these powerful machines was essential, because the curved ray tracing discretizes the curves using straight stretches, and therefore it is necessary to make the intersection test of each stretch with the objects of the scene, generating much more calculations than a conventional ray tracer. As the scenes used are geometrically simple, we have not employed any acceleration method. For a general case, it would be necessary to use some acceleration technique to reduce the computational cost, like the method of space subdivision in voxels [8].

The rendering times for the 200 frames of each of the sunset animations were 14.1 seconds for the split sun scene, 421.4 for the flattened sun scene (about seven minutes) and 4358.7 seconds for the double sun scene (about 72 minutes). In all these cases we used 32 of the T3E's processors in parallel. Each frame had a size of 200 by 200 pixels.

For the split sun scene we did not use the curved ray tracing, since the change of the index of refraction is discrete at the discontinuity between layers. We therefore made a custom program to generate the animation, therefore keeping rendering times low. The double sun scene took much longer because the integration steps obtained through the Richardson extrapolation algorithm were very small in the vicinities of the earth in order to correctly obtain the curvature of the ray.

The parallelization method used was based on the procedure called processor farm [13], which consists of a controller processor which assigns tasks to various worker processors as they finish the previous ones. Although the tasks in a ray tracer usually correspond to portions of the image, in our case, the tasks were defined to calculate entire frames, which is generally a better approach for animations. In the implementation we used the standard MPI [14], suitable for the construction of parallel programs on machines with distributed memory.

5. Conclusions

In this paper, we have succeeded in displaying various natural phenomena that are impossible to generate using the traditional methods of straight ray tracing: distortions of the spherical shape of the sun during sunsets (split sun, flattened sun and double sun).

To achieve this, we have solved numerically, in an adequate way, the differential equation of the ray path in an inhomogeneous medium.

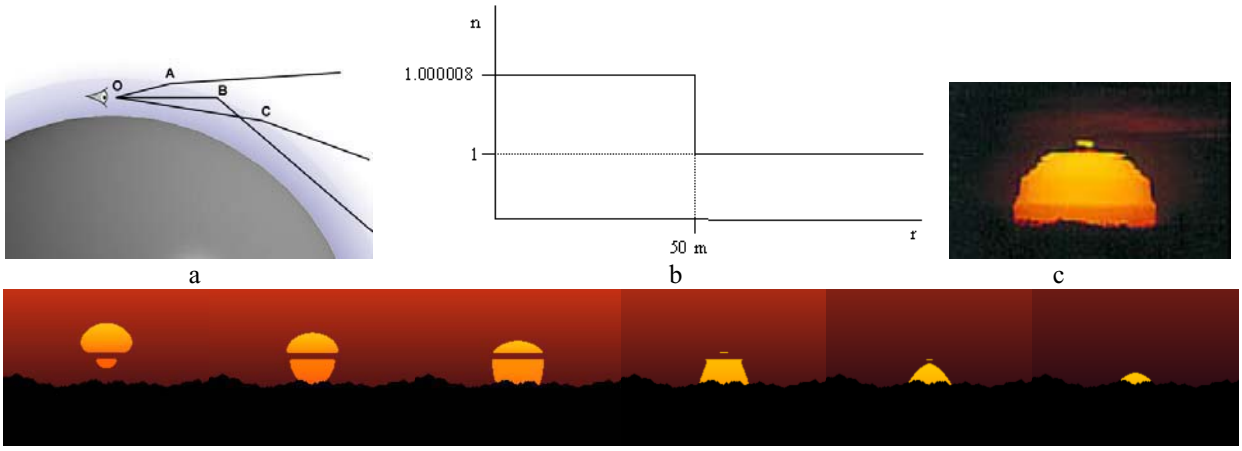

Figure 1. a: representation of the split sun effect, b: distribution of the index of refraction, c: real picture of the effect. d: several frames of the resulting animation

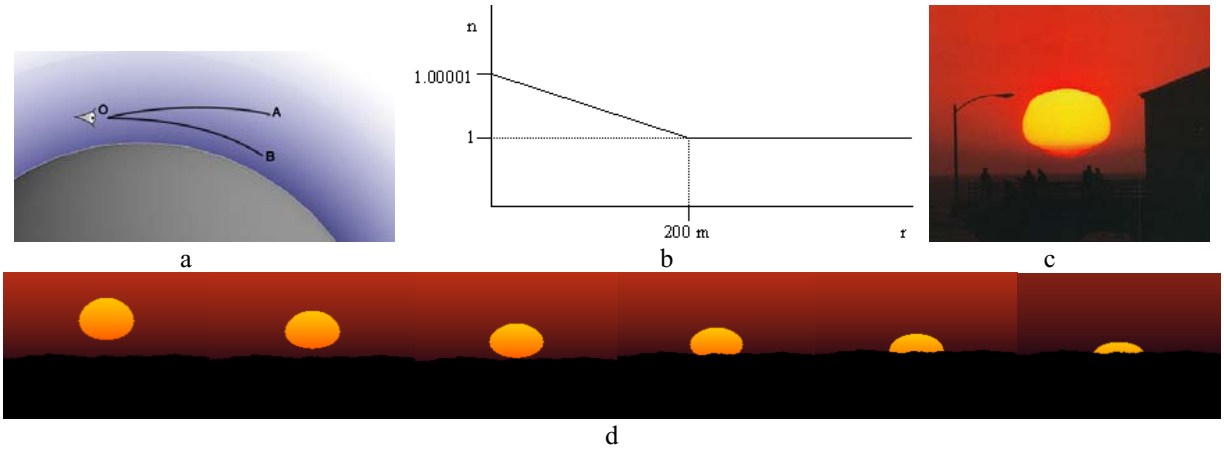

Figure 2. a: representation of the flattened sun effect, b: distribution of the index of refraction, c: real picture of the effect, d: several frames of the resulting animation.

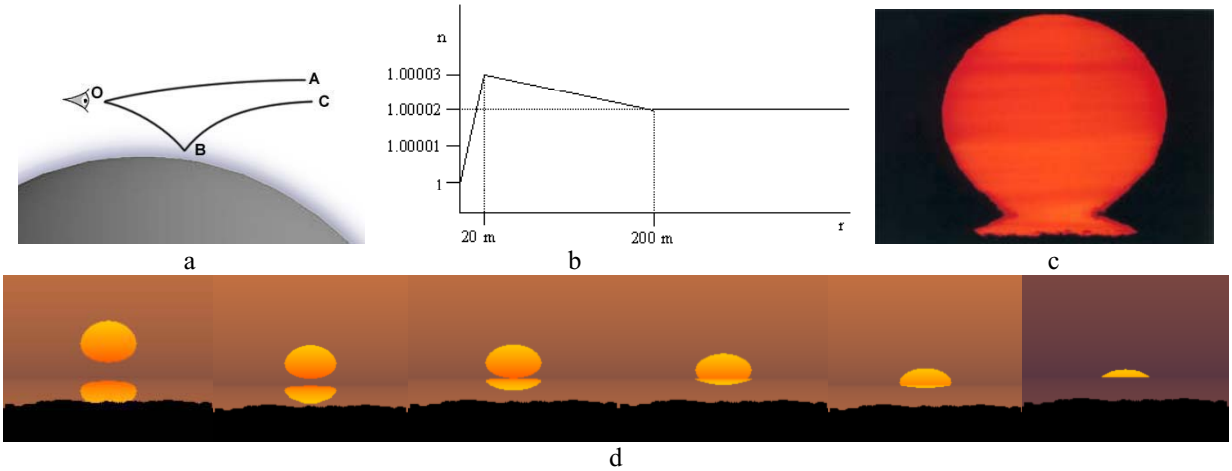

Figure 3. a: representation of the double sun effect, b: distribution of the index of refraction, c: real picture of the effect, d: several frames of the resulting animation.

Our method is valid independently of the distribution of the index of refraction of the medium, overcoming the limitations imposed by previous methods.

Finally, even though we have only worked on inhomogeneous atmospheres, our technique could be generalized, with the proper changes, to any non-homogeneous medium.

6. Future work

All the scenes have been generated using fixed colours for the objects, obtained from photographic textures. A more adequate process for more complex scenes would be to trace curved rays from the light sources and then to trace them from the point of view. For each intersection point, we would calculate the shading using the information obtained in the first stage. Several approaches could be used that involve different global illumination techniques: some references can be found in [15], [16], [17], [18].

The method is also being applied to simulate other atmospheric phenomena such as the distortion of the line of horizon, mirages or the visual perturbations owed to turbulences in the air caused by fire.

7. Acknowledgements

We would like to thank José María Franco, professor of the Department of Applied Mathematics of the University of Zaragoza, for his explanations concerning the convergence of the Euler's method. The authors would also like to thank CESCA, for letting us use some of its computers.

This research was partly done under the sponsorship of the Comisión Interministerial de Ciencia y Tecnología (CICYT), projects TIC-95-0614-C03-01, TIC 2000-0426-P4-02 and TIC 2001-2392-C03-02.

The third author has made use of a research grant and a stay of two months at the Edinburgh Parallel Computing Centre of the University of Edinburgh, within the program of Training and Mobility of Researchers.

8. References

[1] D. Phillips Mahoney. "Animating nature". *Computer Graphics World*, December 1996.

[2] F. K. Musgrave. "Methods for realistic landscape rendering". *PhD thesis*, Yale University, November 1993.

[3] T. Nishita. "Light scattering models for the realistic rendering of natural scenes". *Rendering Techniques 98*, pp. 1-10, 1998.

[4] M. Berger, T. Trout. "Ray tracing mirages". *IEEE Computer Graphics and Applications*, 11(5), pp. 36-41, May 1990.

[5] F. K. Musgrave. "A note on ray tracing mirages". *IEEE Computer Graphics and Applications*, 10(6), pp. 10-12, 1990.

[6] J. Stam, E. Languenou, "Ray tracing in non-constant media". *Proceedings of Rendering Techniques '96*, pp. 225-234, 1996.

[7] Y. A. Kravtsov, Y. I. Orlov, *Geometrical optics of inhomogeneous media*. Springer Verlag, 1990.

[8] E. Groeller. "Nonlinear ray tracing: visualizing strange worlds". *The Visual Computer* 11(5), pp. 263-274, Springer Verlag, 1995.

[9] S. A. Glassner. *Principles of digital image synthesis*. Morgan Kauffman Publishers, Inc. ISBN 1-55860-276-3, 1995.

[10] S. G. Lipston, H. Lipston, D. S. Tannhauser. *Optical physics*. Third edition. Cambridge. ISBN 0 521 43631 1, 1995

[11] E. Hairer, S. P. Norssot, G. Wanner. *Solving ordinary differential equations I: nonstiff problems*. Springer-Verlag, Springer Series on Computational Mathematics, Vol. 8. ASIN: 0387171452, 1993.

[12] J. Fisher. *Introduction to the Cray T3D at EPCC* EPCC, University of Edinburgh, 1997.

[13] S. Green. *Parallel processing for computer graphics*. MIT Press, Cambridge, MA. ISBN:0-262-57087-4, 1991.

[14] "MPI: A message-passing interface standard". University of Tennessee, 1995.

[15] J. Arvo. "Backward ray tracing". Developments in ray tracing, course notes of *SIGGRAPH'86*, volume 12, 1986.

[16] H. W. Jensen. "Rendering caustics on non-lambertian surfaces". *Graphics Interface 96*, pp. 116-121, 1996.

[17] H. W. Jensen. *Realistic image synthesis using photon mapping*. AK Peters, ISBN 1-56881-147-0, 2001.

[18] I. Wald, T.J. Purcell, J. Schmittler, C. Benthin P. Slusallek, "Realtime Ray Tracing and its use for Interactive Global Illumination", *Eurographics 2003 State of the Art Reports*, 2003.